

# DESIGN AND FABRICATION OF DESKTOP CNC MILLING MACHINE

Tyler Woodard<sup>1</sup>, Andrew Honeycutt<sup>2</sup>, John Greene<sup>1</sup>, and Tony Schmitz<sup>1,2</sup>

<sup>1</sup>Mechanical, Aerospace, and Biomedical Engineering Department

University of Tennessee

Knoxville, TN, 37996, USA

<sup>2</sup>Manufacturing Demonstration Facility

Oak Ridge National Laboratory

Oak Ridge, TN, 37830, USA

## INTRODUCTION

This paper describes the design and fabrication for a three-axis computer numerically controlled (CNC) desktop milling machine. Currently, there is a high-cost barrier to entry for this technology. Limiting the accessibility of manufacturing experience may lead to an underdeveloped workforce and exacerbate existing machining workforce challenges. The primary goal of this machine is to provide a low-cost option to high school educators for CTE programs. The intent of the machine tool and supporting curriculum is to introduce machining and machining science to the next generation of manufacturers.

The design goals are ease of assembly, low cost, open-source motion control, and open-source interface software to achieve the desired machine tool performance. Performance goals are selected to support the training course supplied with the machine tool. This includes the ability to machine aluminum alloys with sufficient accuracy and surface finish to enable assembly of components for relevant and interesting demonstrations. The machine performance was evaluated through error motion measurements and cutting tests. Design and assembly details are provided.

## DESIGN DESCRIPTION

The machine design consists of a vertical spindle orientation perpendicular to the worktable. 6061-T6 aluminum alloy is used for all the manufactured machine tool components to provide ease of manufacturing and distribution. The component sizes were selected to enable fabrication from standard aluminum bar stock. The work volume is 152 mm x 254 mm x 177 mm; see Figure 1. All axes consist of two HGR20 linear rails paired with SFU1605 ball screws for translation. The ball screw is driven by a Nema 23 stepper motor with 2.45 N-m of holding torque. These motors provide 1.8 degrees per step and are micro stepped to 0.9 degrees for increased

resolution with sufficient operating torque. Resolution for a single axis was calculated as 3  $\mu$ m based on the ball screw pitch and steps per revolution. A 1.5 kW air cooled spindle, from Huajiang, was selected based on price, availability, and capability. This spindle operates on a variable frequency drive so only a standard 110VAC outlet is required.

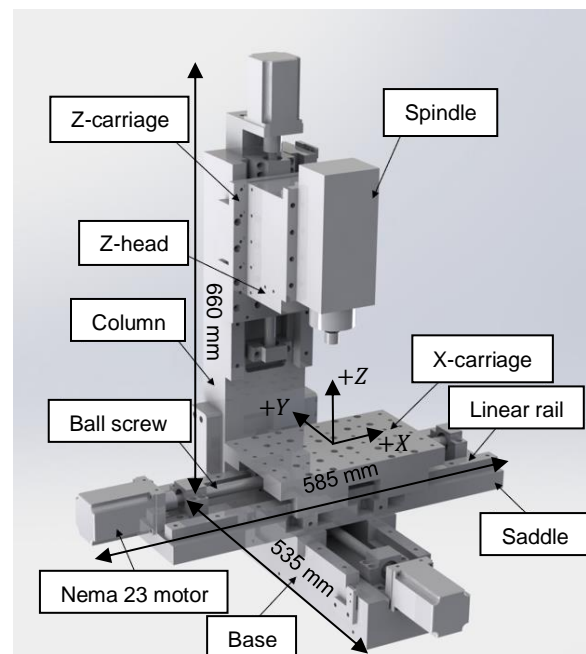


FIGURE 1. Desktop machine model.

The motion control system consists of the open-source software G-Code Reference Block Library (GRBL). This software is intended for microcontrollers, so a Teensy 4.1 board was selected. This board includes an ARM Cortex-M7 at 600 MHz and 8 MB of RAM which limits data starvation of the controller for larger programs. The Teensy 4.1 also includes a safety door switch pin to ensure safe operation. GRBL is not a stand-alone controller, so it is coupled with IO Sender. IO Sender is an open-source software

that sends blocks of g-code to the microcontroller running GRBL from any standard laptop with USB.

The microcontroller and other electrical components are packaged in a 410 mm × 310 mm × 180 mm junction box. DM556 digital stepper drivers actuate each axis at a maximum feed of 1500 mm/min. The motion control operates at 48VDC through a 110VAC power supply. Star-point grounding through a terminal bus bar was implemented during the wiring process to ensure proper grounding. With proper grounding, the electromagnetic interference from the variable frequency drive and stepper drive is reduced within the signal wires. The wiring diagram for the control components is shown in Figure 2. This configuration is compatible with commercial computer aided manufacturing (CAM) software, such as Fusion 360, which supports curriculum development and distribution.

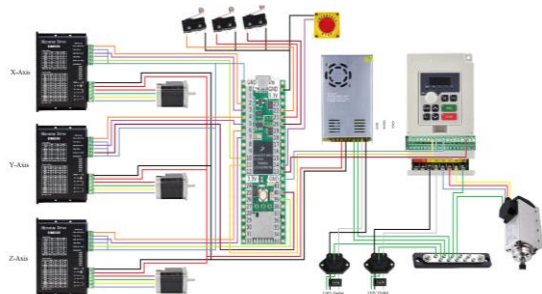


FIGURE 2. Wiring diagram.

### MANUFACTURING AND ASSEMBLY

Each designed component was machined on a Haas VF-4 CNC machining center. Selection of 6061-T6 aluminum as the material reduced the manufacturing time. The longest cycle time was 30 minutes for the X-axis saddle.

The first assembly step was to mount the linear rails parallel to one another. This was done with gauge blocks initially, followed by sweeping the rail with a test indicator. The ball screw was then mounted parallel with the rails and was coupled to the stepper motor. Each axis was tested for binding before proceeding. Bolted connections were selected for these assembly steps, so assembly can be completed with standard tooling.

After assembly, the machine tool axes were squared using a 1-2-3 setup block and test indicator; see Figure 3.

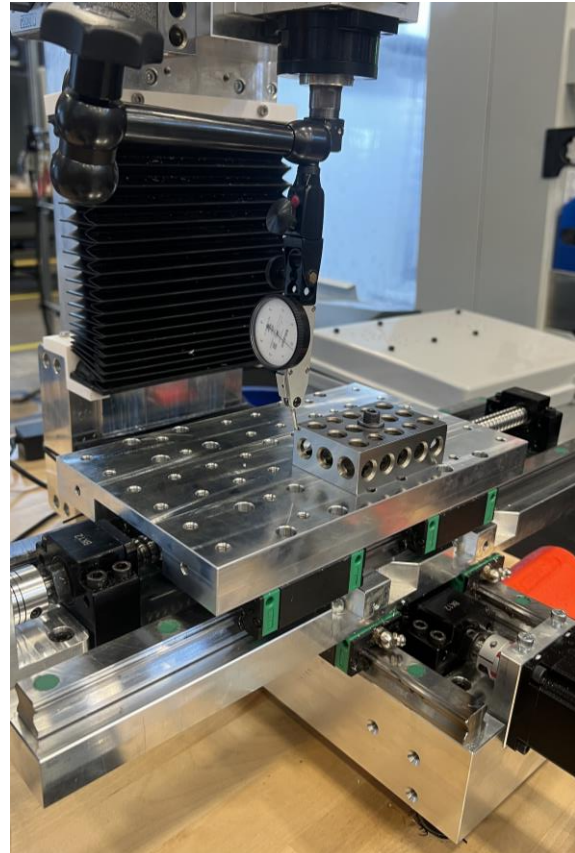


FIGURE 3. Squaring process setup.

The squaring process began with sweeping the setup block's longest dimension parallel with the X-axis travel. Next, the saddle (Y-axis) was adjusted without disturbing the parallelism of the X-axis to the setup block. The result of adjustment was approximately 10  $\mu\text{m}$  of deviation in perpendicularity across 50.8 mm. Next, the Z-axis was adjusted to be perpendicular to the X-Y plane. This was completed in a similar manner with the setup block placed vertically. Adjustments were made with shim stock inserted at the interface of the column and base. The Z-axis nod was adjusted to approximately 3  $\mu\text{m}$  deviation across 50.8 mm with similar results for the Z-axis tilt. The final step of ensuring the machine is assembled properly was aligning the spindle with the Z-axis. This was completed by mounting a gauge pin in the spindle testing its radial error motion using an indicator. Measurements performed in both the X and Y directions until the spindle was aligned. The results were approximately 3  $\mu\text{m}$  of deviation across 19 mm for the  $E_{AX}$  direction (spindle nod) and 20  $\mu\text{m}$  across 19 mm for the  $E_{BX}$  direction (spindle tilt); see Figure 5. There are current efforts to update the design to enable improved

adjustment of the spindle alignment. The larger deviation is observed in the performance evaluation.

### PERFORMANCE EVALUATION

Two tests were conducted to evaluate the performance of the machine tool design. The first test was measuring the X-axis error motions to find the typical results for the machine axes. Figure 4 displays the Renishaw XL-80 laser interferometer setup for the linear error motion measurement of the X-axis (220 mm of travel with increments of 20 mm). All measurements were compensated for pressure, humidity, and temperature. The error motions are shown in Figure 5.

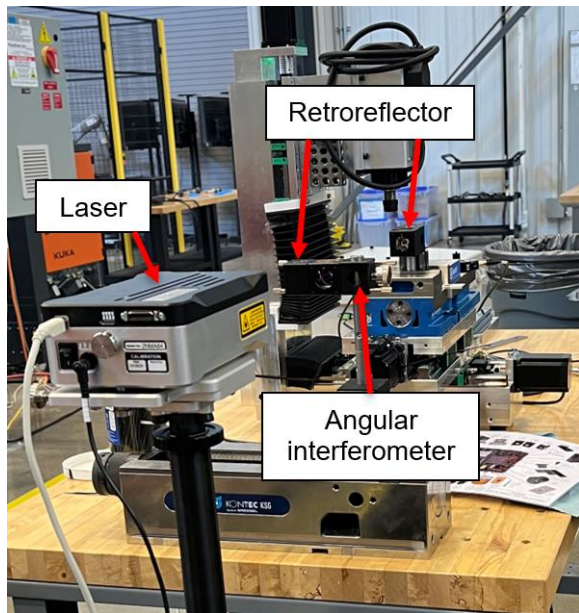


FIGURE 4. Linear error motion measurement setup.

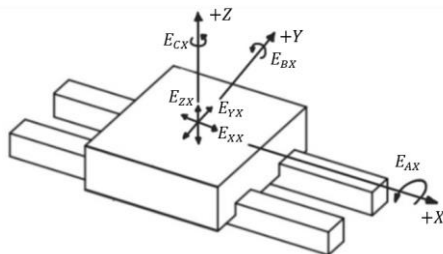


FIGURE 5. Error motions for X-axis [4].

The initial measurements showed 13  $\mu\text{m}$  of backlash in the axis. GRBL provides backlash compensation, so this was integrated into the controller before the final measurements were completed. Linear positioning, straightness error, and angular error values are reported per ASME

B5.54. Figures 6-10 display the data after slope removal. Each figure contains three test runs in the positive and negative directions denoted by the +/- symbols in the legend. As shown in Figure 6, the bidirectional positioning error,  $E_{XX}$ , was 30  $\mu\text{m}$  after slope removal to account for laser misalignment. The bidirectional positioning repeatability was 10.5  $\mu\text{m}$  with a reversal error of 4.8  $\mu\text{m}$ .

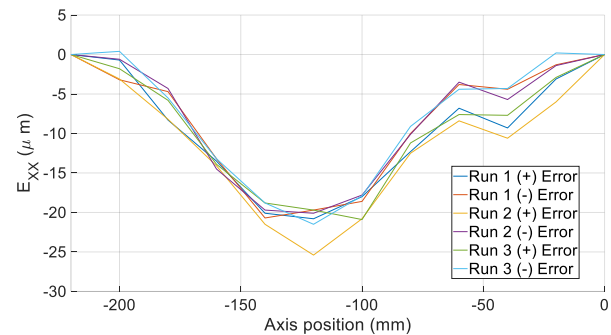


FIGURE 6. X-axis linear positioning error  $E_{XX}$ .

Angular error motions were measured with a similar setup. However, a retroreflector pair was placed on the moving table to determine angular deviation. Figure 7 shows the angular error motion about the Y-axis (B-axis). The measured angular error,  $E_{BX}$ , was 194.3  $\mu\text{rad}$  bidirectional with reversal error of 4.5  $\mu\text{rad}$ .

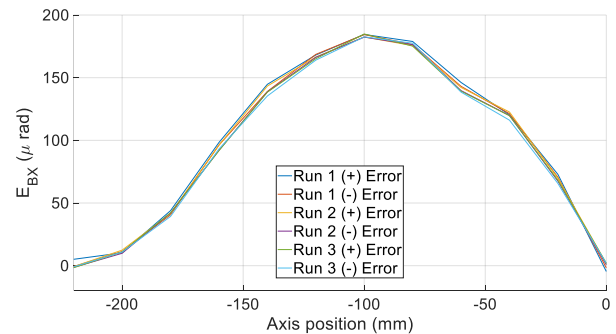


FIGURE 7. X-axis angular error motion  $E_{BX}$ .

Angular error motion about the Z-axis (C-axis),  $E_{CX}$ , was measured as 108.9  $\mu\text{rad}$  bidirectional with a reversal error of 2.7  $\mu\text{rad}$ . Results from the  $E_{CX}$  measurement is shown in Figure 8. The angular error motion about the X-axis,  $E_{AX}$ , was not available for the experimental setup.

Straightness errors were measured using a straightness mirror and Wollaston prism. The straightness mirror was placed on the translating bed. The straightness error motion,  $E_{ZX}$ , was 32.5

$\mu\text{m}$  as seen in Figure 9. The straightness error motion in the Y-direction is shown in Figure 10 and was  $43.2 \mu\text{m}$ .

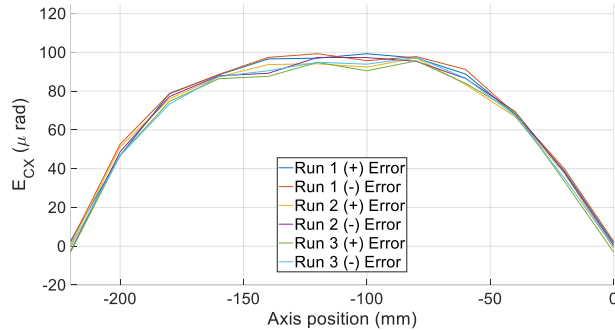


FIGURE 8. X-axis angular error motion  $E_{CX}$ .

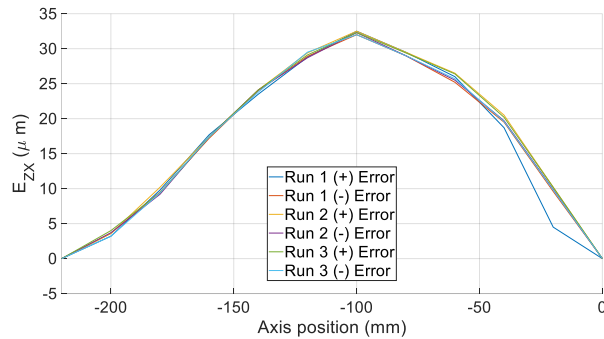


FIGURE 9. X-axis straightness error  $E_{ZX}$ .

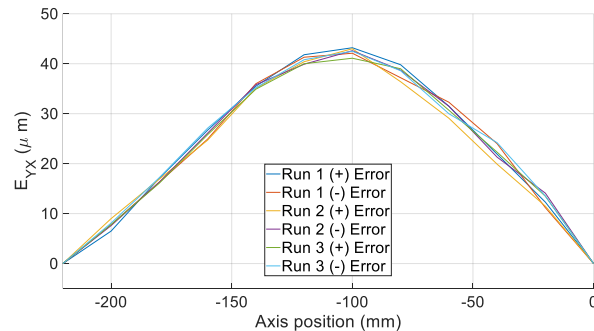


FIGURE 10. X-axis straightness error  $E_{YX}$ .

These error motion measurements are considered typical since all axes are assembled with nearly identical parts. Comparisons between this data and commercially available machine tools will be performed as development continues. Table 1 summarizes the error motion measurements per the ASME standard.

TABLE 1. Error motion measurements [1].

Error motion	Bidirectional error	Bidirectional repeatability	Reversal
$E_{XX}$	$30.0 \mu\text{m}$	$10.5 \mu\text{m}$	$4.8 \mu\text{m}$

$E_{YX}$	$45.5 \mu\text{m}$	N/A	N/A
$E_{ZX}$	$35.6 \mu\text{m}$	N/A	N/A
$E_{BX}$	$194.3 \mu\text{rad}$	$15.0 \mu\text{rad}$	$4.5 \mu\text{rad}$
$E_{CX}$	$108.9 \mu\text{rad}$	$18.6 \mu\text{rad}$	$2.7 \mu\text{rad}$

The second test was the circle diamond square machining test from ISO 10791-7 2020. The M1 test piece type was selected to evaluate the positioning and contouring performance of the machine tool, as well as the squareness between axes. The largest size that fits on the machine tool was an  $80 \text{ mm} \times 80 \text{ mm}$  nominal test piece. A fixture was designed to locate the part at the center of the X-Y plane. The design enables the fixture to be removed from the machine tool without removing the test piece from the fixture after machining. This minimizes the influence of test piece distortion due to clamping and is recommended by the standard. Part blanks for the  $80 \text{ mm}$  test piece were prepped on a Haas VF-4 CNC machining center. Figure 11 shows the test part details.

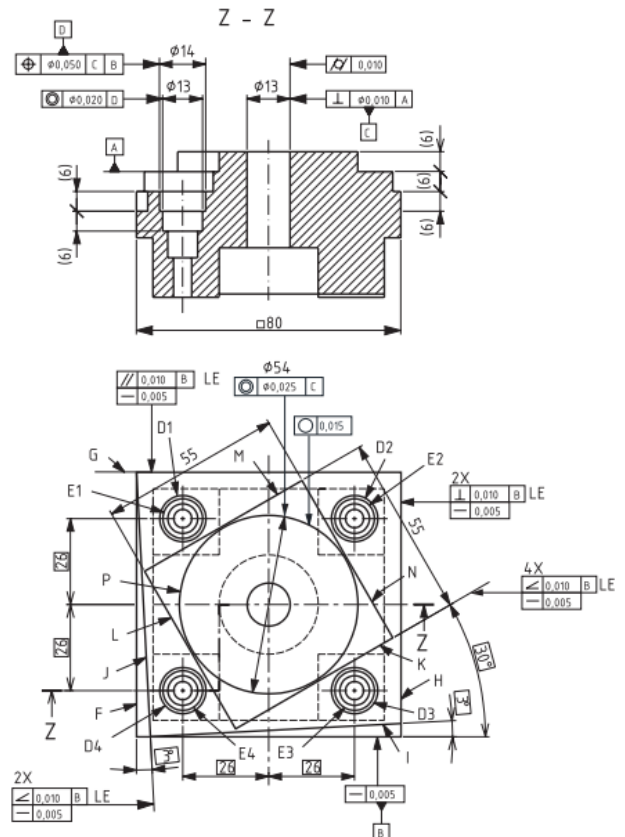


FIGURE 11. Test piece ISO 10791-7, M1\_80 (dimensions in mm) [3].

The material was 6061-T6 aluminum. A  $6.35 \text{ mm}$  diameter, three flute, solid carbide bull nose end

mill was selected for all cutting operations on the test piece. This tool had a zirconium nitride coating that is compatible with the test piece material. Stable machining parameters were selected, and an air blast was supplied for chip removal; cutting fluid was not used in these tests. For every cutting operation, climb milling was implemented. Contouring roughing parameters were: 6 mm axial depth, 0.508 mm radial depth, 1200 mm/min linear feed rate, and 24,000 rpm spindle speed. The roughing parameters for the boring operations were: 254 mm/min ramp feed rate and 24,000 rpm spindle speed. For all finishing operations, the radial depth was reduced to 0.254 mm. Otherwise, the parameters were the same except for the bored (E), counter bored holes (D), and central hole (C) across different test pieces. Figure 12 shows the final part after all operations were completed on the desktop mill. The last consideration for the cutting parameters was the approach direction for the holes E and D. These holes were approached in the positive and negative direction of the positioning axes, respectively. The reversal error is therefore included within the final part dimensions.

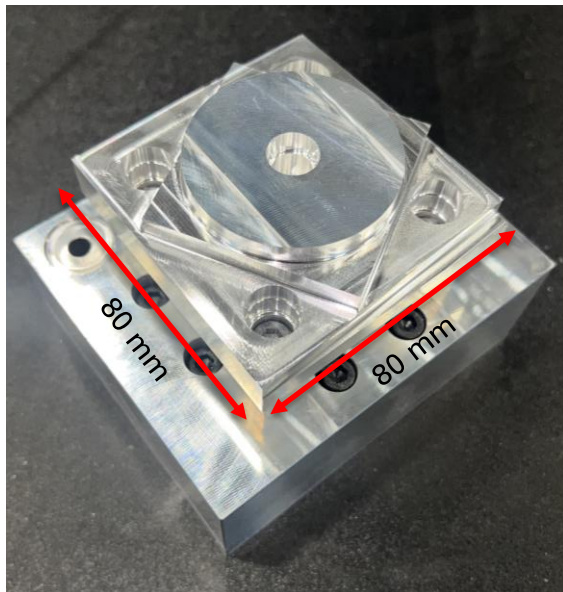


FIGURE 12. Final test piece and fixture.

The test piece was measured on a ZEISS Duramax coordinate measuring machine (CMM). The program for the CMM measurements was based on the drawing in Figure 11. For straight sides on the part, a minimum of 10 points is recommended to obtain straightness, perpendicularity, and parallelism deviations. The CMM program measured every feature at 3 mm/s with a step width of 0.1 mm. A similar

recommendation was made and met for the roundness and cylindricity. The results from the CMM measurements are provided in Table 2, which compares the tolerances from the standard to the measured values. Two test pieces were machined and measured.

TABLE 2. CMM results from the second test piece.

Object	Characteristic	Tol [mm]	Measured [mm]
Central hole	Perpendicularity: C-A	0.010	0.063
	Cylindricity: C		0.077
Square	Straightness: B	0.005	0.007
	Straightness: F		0.007
	Straightness: G		0.012
	Straightness: H	0.010	
	Perpendicularity: H-B	0.010	0.035
	Perpendicularity: F-B		0.061
	Parallelism: G-B		0.029
Diamond	Straightness: K	0.005	0.015
	Straightness: L		0.016
	Straightness: M		0.017
	Straightness: N	0.016	
	Angularity: K-B	0.010	0.022
	Angularity: L-B		0.035
	Angularity: M-B		0.022
	Angularity: N-B		0.019
Circle	Roundness: P	0.015	0.031
	Concentricity: P-C	0.025	0.024
Sloping faces	Straightness: I	0.005	0.010
	Straightness: J		0.011
	Angularity: I-B	0.010	0.013
	Angularity: J-B		0.057
Bored holes	Position: D1-C	0.050	0.023
	Position: D2-C		0.024
	Position: D3-C		0.125
	Position: D4-C		0.056
	Concentricity: E1-D1	0.020	0.020
	Concentricity: E2-D2		0.042
	Concentricity: E3-D3		0.031
	Concentricity: E4-D4		0.030

The CMM measurements show that the machine capabilities are similar to the standard's tolerances but exceed the recommended value in some instances. Larger deviations were examined. The large value in perpendicularity of datum C to plane A can be explained by the squaring process of the machine tool. The larger squareness error was observed for  $E_{BX}$  of 20  $\mu\text{m}$  across 19 mm during assembly. With the spindle's  $E_{BX}$  being out of alignment, the perpendicularity of the cylinder feature to the

plane will illuminate this misalignment. The cylindricity of datum C showed approximately 63  $\mu\text{m}$  of deviation from the nominal value. This feature was machined differently on the first test piece and the cylindricity was measured as 11  $\mu\text{m}$ . The change in the finishing tool path was the radial and axial engagement of the tool. Datum C on the first test piece was machined with a helical boring operation at a feed rate of 356 mm/min and radial engagement of 0.254 mm. The second test piece was machined in one pass at 6 mm axial depth. More testing will be done on the effects of the finishing pass parameters for this machine tool.

Single axis motion straightness deviation of the square faces deviated from the tolerance by approximately 5  $\mu\text{m}$ . The synchronized axis motion for the diamond feature showed an increase in deviation which was expected. Perpendicularity of the square feature revealed how well the machine was assembled. These features are across 80 mm and the squaring process showed 10  $\mu\text{m}$  of deviation across 50.8 mm. This matches with the CMM results except that side F is slightly worse at 0.061 mm.

The positions of the bored holes are out of tolerance of 20  $\mu\text{m}$  due to the linear positioning error of 30  $\mu\text{m}$ . The overall trend from the cutting test show that the machine tends to be within tolerance in most cases with no deviation larger than 0.125 mm.

## **ACKNOWLEDGEMENTS**

The authors acknowledge support from the NSF Engineering Research Center for Hybrid Autonomous Manufacturing Moving from Evolution to Revolution (ERC-HAMMER) under Award Number EEC2133630.

## **REFERENCES**

- [1] ASME B5.54, *Methods for Performance Evaluation of Computer Numerically Controlled Machining Centers*. New York, N.Y: 2005
- [2] ISO 10791-1, *Test conditions for machining centres — Part 1: Accuracy of finished test pieces*. Switzerland: 2020
- [3] ISO 230-1, *Test code for machine tools — Part 1: Geometric accuracy of machines operating under no-load or quasi-static conditions*. Switzerland: 2012
- [4] ISO 230-2, *Test code for machine tools —*

*Part 2: Determination of accuracy and repeatability of positioning of numerically controlled axes*. Switzerland: 2014